

# Magnetic properties of spin diluted iron pnictides from $\mu$ SR and NMR in $\text{LaFe}_{1-x}\text{Ru}_x\text{AsO}$

Pietro Bonfà<sup>1</sup>, Pietro Carretta<sup>1</sup>, Samuele Sanna<sup>1</sup>, Gianrico Lamura<sup>2</sup>, Giacomo Prando<sup>1,3</sup>, Alberto Martinelli<sup>2</sup>, Andrea Palenzona<sup>2</sup>, Matteo Tropeano<sup>2</sup>, Marina Putti<sup>2</sup> and Roberto De Renzi<sup>4</sup>

<sup>1</sup> Department of Physics “A. Volta”, University of Pavia-CNISM, I-27100 Pavia, Italy

<sup>2</sup> CNR-SPIN and Università di Genova, I-16146 Genova, Italy

<sup>3</sup> Department of Physics “E. Amaldi”, University of Roma Tre-CNISM, I-00146 Roma, Italy and

<sup>4</sup> Department of Physics, University of Parma-CNISM, I-43124 Parma, Italy

The effect of isoelectronic substitutions on the microscopic properties of  $\text{LaFe}_{1-x}\text{Ru}_x\text{AsO}$ , for  $0 \leq x \leq 0.8$ , has been investigated by means of  $\mu$ SR and  $^{139}\text{La}$  NMR. It was found that Ru substitution causes a progressive reduction of the Néel temperature ( $T_N$ ) and of the magnetic order parameter without leading to the onset of superconductivity. The temperature dependence of  $^{139}\text{La}$  nuclear spin-lattice relaxation rate  $1/T_1$  can be suitably described within a two-band model. One band giving rise to the spin density wave ground-state, while the other one is characterized by weakly correlated electrons. Fe for Ru substitution yields to a progressive decrease of the density of states at the Fermi level close to the one derived from band structure calculations. The reduction of  $T_N$  with doping follows the predictions of the  $J_1 - J_2$  model on a square lattice, which appears to be an effective framework to describe the magnetic properties of the spin density wave ground-state.

PACS numbers: 76.75.+i, 75.10.Jm, 74.90.+n, 76.60.Es

## I. INTRODUCTION

The recent discovery of high temperature superconductivity nearby the disruption of magnetic order in Fe-based compounds<sup>1</sup> has stimulated the scientific community to further consider the role of magnetic excitations<sup>2</sup> as a possible candidate for the pairing mechanism. In order to address this point an appropriate modellization of the microscopic magnetic properties of the Fe based superconductors and of their parent compounds is necessary. In the phase diagram of iron pnictides superconductivity appears to compete with a commensurate spin density wave (SDW) magnetic order<sup>3</sup> characterized by a reduced magnetic moment.<sup>4</sup> The magnitude of this moment is much lower than that evaluated from band structure calculations,<sup>5</sup> possibly due either to the strong electronic correlations, not appropriately taken into account in those calculations, and/or from frustration effects.<sup>6</sup>

When the SDW phase is suppressed, by chemical substitution or by applying high pressures, superconductivity is usually recovered.<sup>7-9</sup> In fact, in  $A(\text{Fe}_{1-x}\text{Ru}_x)_2\text{As}_2$  ( $A=\text{Sr}, \text{Ba}$ ) the substitution of Fe by Ru suppresses the magnetic ordering for  $x \rightarrow 0.3$  and leads to bulk superconductivity for  $0.2 < x < 0.4$ .<sup>10-13</sup> On the other hand, it has been shown that in  $\text{PrFe}_{1-x}\text{Ru}_x\text{AsO}$ ,<sup>14</sup> in spite of an analogous disruption of the SDW ordering for  $x \simeq 0.6$ , no superconductivity is found up to the full Ru substitution. Indeed band structure calculations for  $\text{REFe}_{1-x}\text{Ru}_x\text{AsO}$  show that the electronic structure around the Fermi level is actually only slightly affected by Ru substitution<sup>15</sup> and that only a minor charge doping takes place, even in the presence of very large Ru contents.<sup>15</sup> This means that in this system the Fe/Ru substitution is effectively isoelectronic and accordingly no relevant modification of the electronic ground-state is observed. Furthermore it

has been predicted<sup>15</sup> that the Ru atoms do not sustain any magnetic moment suggesting that  $\text{REFe}_{1-x}\text{Ru}_x\text{AsO}$  should be considered as a spin-diluted system.

In order to understand which is the effect of Ru substitution in the 1111 family of iron pnictides we have performed  $\mu$ SR and  $^{139}\text{La}$  NMR measurements in  $\text{LaFe}_{1-x}\text{Ru}_x\text{AsO}$ . A progressive reduction of the Néel temperature ( $T_N$ ) and of the magnetic order parameter is observed with increasing  $x$ . Both quantities eventually vanish for  $x \rightarrow 0.6$  without leading to the onset of superconductivity, at least up to  $x = 0.8$ . The temperature dependence of  $^{139}\text{La}$  nuclear spin-lattice relaxation rate  $1/T_1$  can be suitably described within a two-band model, one giving rise to the SDW ground-state, while the other one characterized by a Fermi-gas behaviour. Ru for Fe substitution yields to a progressive decrease of the density of states at the Fermi level, a trend which is quite consistent with band structure calculations. The low temperature behaviour of  $1/T_1$  in the ordered phase and the reduction of  $T_N$  with doping can both be described within the  $J_1 - J_2$  model on a square lattice and indicate that  $\text{LaFe}_{1-x}\text{Ru}_x\text{AsO}$  behaves as a spin-diluted system with competing exchange interactions. This observation suggests that this model provides an effective framework to suitably describe the role of frustration in the iron pnictides.<sup>6,16</sup>

## II. TECHNICAL ASPECTS AND EXPERIMENTAL RESULTS

The experiments were performed on polycrystalline  $\text{LaFe}_{1-x}\text{Ru}_x\text{AsO}$  ( $0 \leq x \leq 0.8$ ) samples prepared as described in Ref 17. Structural characterization was performed by X-ray powder diffraction at room temperature and Rietveld refinement was carried out on selected

diffraction patterns. Microstructure was inspected by scanning electron microscopy. Transport measurements show a decrease in the resistivity  $\rho$  with increasing Ru content and a shift to low temperature of the characteristic anomaly in  $d\rho/dT$  at  $T_N$ .<sup>17</sup> The magnetic susceptibility  $\chi$  derived from SQUID magnetization measurements showed an analogous behaviour of the peak in  $d\chi/dT$  at  $T_N$ , shifting to lower temperatures with increasing  $x$ . However, for  $x \geq 0.4$  the peak progressively smeared out and eventually for  $x \rightarrow 0.6$  the susceptibility showed basically a Curie-Weiss behaviour.

Zero field (ZF)  $\mu$ SR experiments have been performed at PSI with GPS spectrometer. For  $T > T_N$ , the muon asymmetry is characterized by a decay which progressively increases with decreasing temperature. Below  $T_N$ , at low Ru contents, well defined oscillations are observed (Fig.1), evidencing the presence of a magnetic order. For  $x \geq 0.3$  (Fig.1) these oscillations are markedly damped due to the increase in the local field distribution at the muon site.

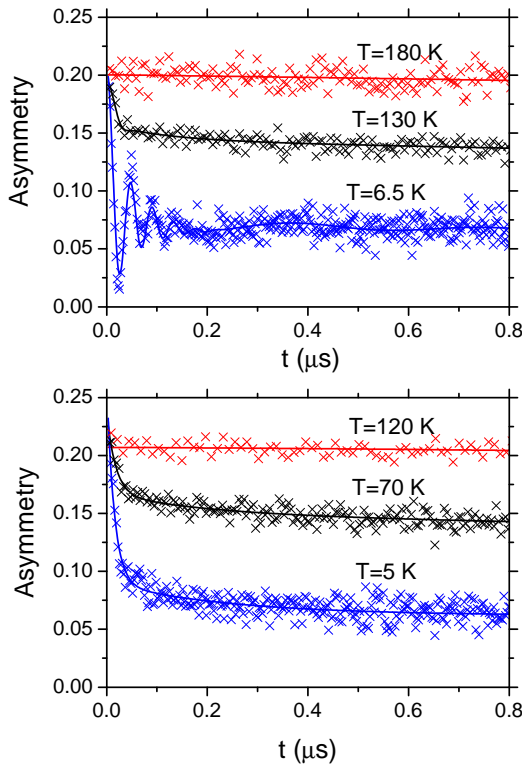


FIG. 1: Time evolution of the muon asymmetry in  $\text{LaFe}_{1-x}\text{Ru}_x\text{AsO}$  for  $x = 0.1$  (top) and for  $x = 0.4$  (bottom) at three selected temperatures. The solid lines are the best fits according to Eq.1.

Accordingly, for  $x \leq 0.3$  the asymmetry could be fitted to the sum of a fast and a slow oscillation plus a non-oscillating term, namely

$$A(t) = A_1 e^{-\lambda_1 t} f(\gamma_\mu B_1^\mu t) + A_2 e^{-\lambda_2 t} f(\gamma_\mu B_2^\mu t) + A_{\parallel} e^{-\lambda_{\parallel} t}, \quad (1)$$

where  $\gamma_\mu$  is the muon gyromagnetic ratio,  $B_{1,2}^\mu$  is the local field at the muon sites<sup>18,19</sup>  $i = 1$  or  $2$  and  $\lambda_{1,2}$

are the corresponding decay rates. As can be seen from Fig.1 the amplitude of the fast oscillating component is significantly larger than the one of the slow oscillating term. The fast oscillating signal could be reproduced by  $f(\gamma_\mu B_1^\mu t) = \cos(\gamma_\mu B_1^\mu t + \phi)$  for  $x < 0.3$ . At higher Ru contents  $f(\gamma_\mu B_1^\mu t) = J_0(\gamma_\mu B_1^\mu t)$ , with  $J_0$  the zeroth order Bessel function. For  $T \ll T_N$ , for  $x < 0.6$ , one finds that  $A_{\parallel}$  is  $1/3$  of the total asymmetry, as expected for fully magnetically ordered powders.<sup>20</sup> Then it is possible to estimate the temperature dependence of the magnetic volume fraction  $v_M(T) = (3/2)(1 - A_{\parallel}(T))$  from the temperature dependence of  $A_{\parallel}(T)$ . The fraction  $v_M(T)$  is shown in Fig. 2 for different doping levels. One notices a fast drop of  $v_M$  for  $T \rightarrow T_N$ , which can be empirically fitted with  $v_M(T) = 0.5(1 - \text{erf}(T - T_N^{av}/\sqrt{2}\Delta_V))$ , where  $T_N^{av}$  represents an average transition temperature. One observes a progressive decrease of  $T_N^{av}$  with  $x$  together with some broadening, likely due to inhomogeneity in the Ru distribution. Notice that for  $x \leq 0.5$  the temperature at which  $v_M$  reaches about 100 % is close to  $T_N$  as determined from resistivity measurements, as it is shown in details in the next section.

The fit of the muon asymmetry for  $x \leq 0.3$  allows one to derive the temperature dependence of the modulus of the local field at the muon  $B_i^\mu(T) = \mathcal{A}_i \langle \mathbf{S} \rangle$ , with  $\mathcal{A}_i$  the hyperfine coupling tensor and  $\langle \mathbf{S} \rangle$  the average Fe spin value, corresponding to the order parameter. In Fig. 3 the temperature dependence of  $B_1^\mu(T)$ , the internal field at the muon site close to FeAs layers,<sup>19</sup> is reported for  $x \leq 0.3$ . One notices a progressive decrease of the Fe magnetic moment with increasing  $x$ .

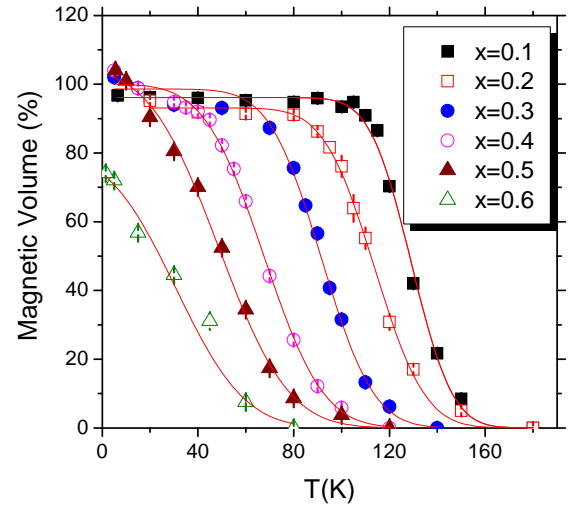


FIG. 2: Temperature dependence of the magnetic volume fraction in  $\text{LaFe}_{1-x}\text{Ru}_x\text{AsO}$ . The solid lines are the best fits according to the phenomenological expression  $v_M(T) = 0.5(1 - \text{erf}(T - T_N^{av}/\sqrt{2}\Delta_V))$ .

<sup>139</sup>La NMR measurements have been carried out by using standard radiofrequency pulse sequences. The spectra of the  $x = 0$  compound was in excellent agreement with the one previously reported by Ishida *et al.*<sup>21</sup> Upon doping one observes that the peaks of the central line progressively smear out and the spectrum gets

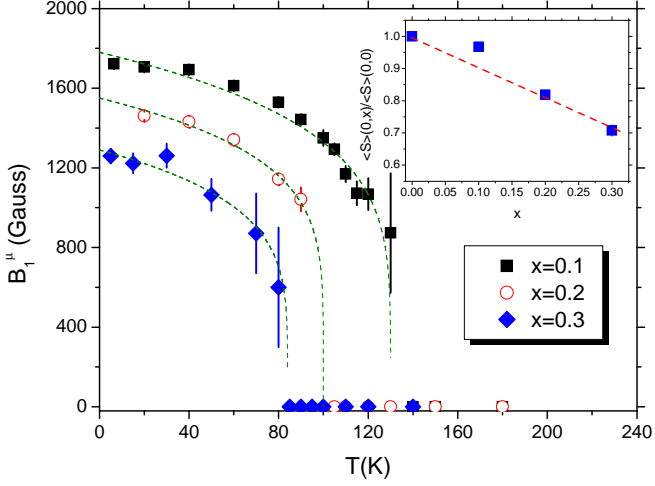


FIG. 3: Temperature dependence of the local field at the muon site 1 in  $\text{LaFe}_{1-x}\text{Ru}_x\text{AsO}$ , for  $0.1 \leq x \leq 0.3$ . The dashed lines are guides to the eye. In the inset the  $x$ -dependence of the  $T \rightarrow 0$  order parameter  $\langle S \rangle (T \rightarrow 0, x) / \langle S \rangle (T \rightarrow 0, 0) = B_1^\mu(T \rightarrow 0, x) / B_1^\mu(T \rightarrow 0, 0)$  is shown. The dashed line is a guide to the eye.

narrower, suggesting a decrease in the electric field gradient at  $^{139}\text{La}$  nuclei and possibly also a change in the paramagnetic shift tensor. The explanation of this phenomenology, however, goes beyond the aim of the present manuscript. Nuclear spin-lattice relaxation rate  $1/T_1$  was measured on the central transition by using a saturation recovery pulse sequence. The recovery of the nuclear magnetization does not follow the trend expected for a magnetic relaxation mechanism<sup>22</sup> by assuming a single  $T_1$  but could rather be fitted by assuming a distribution of  $T_1$ . Hereafter  $T_1$  will be defined as the time at which the recovery law decays to  $1/e$ . The temperature dependence of  $1/T_1$  in  $\text{LaFe}_{1-x}\text{Ru}_x\text{AsO}$  is shown in Fig.4.  $1/T_1$  shows a linear temperature dependence above  $T_N$  and a drop below. The peak at the transition temperature originates from the divergence of critical fluctuations, progressively smeared out by inhomogeneities for increasing  $x$ . Figure 5 displays the temperature dependence of  $1/T_1 T$  on log-linear scales. It is worth noticing that the relaxation rate does not vanish for  $T \rightarrow 0$ , where it tends to a constant,  $x$ -dependent value. The low temperature levelling of  $1/T_1$  has already been observed by Nakai et al. in Ref.23 for the parent  $x = 0$  compound.

### III. ANALYSIS AND DISCUSSION

First we shall concentrate on the effect of Ru doping on the sublattice magnetization and on the density of states at the Fermi level in the light of band structure calculations, performed within the density functional theory (DFT) using the local density approximation (LDA) for the exchange and correlation functional. The band structure was obtained with the SIESTA code,<sup>24</sup> which utilizes a linear combination of atomic orbitals for valence elec-

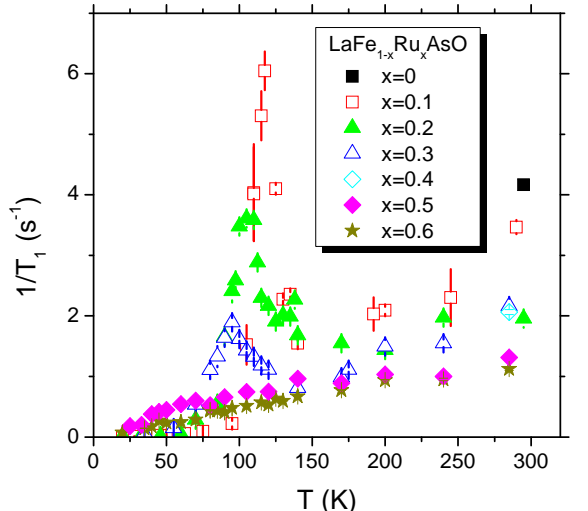


FIG. 4: Temperature dependence of  $^{139}\text{La}$   $1/T_1$  in  $\text{LaFe}_{1-x}\text{Ru}_x\text{AsO}$ , for  $0.1 \leq x \leq 0.6$ , in a 7 Tesla magnetic field.

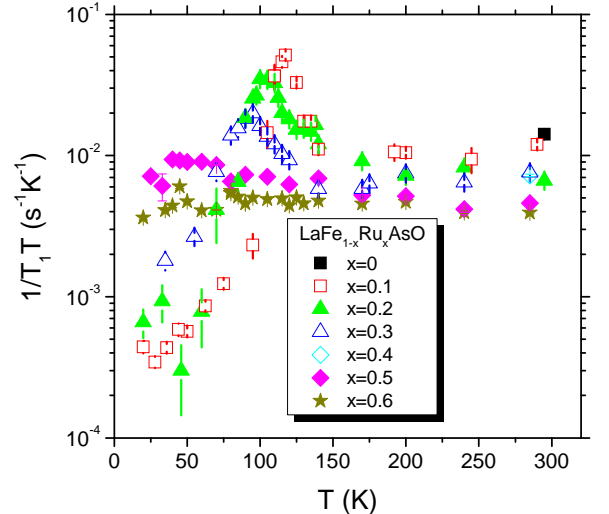


FIG. 5: Temperature dependence of  $^{139}\text{La}$   $1/T_1 T$  in  $\text{LaFe}_{1-x}\text{Ru}_x\text{AsO}$ , for  $0.1 \leq x \leq 0.6$ , in a 7 Tesla magnetic field.

trons and separable norm conserving pseudopotentials with partial corrections for atomic cores. Crystal structures relaxations were performed with periodic boundary conditions. The atomic positions as well as the cell structure were allowed to be optimized in the paramagnetic state by using a conjugate gradient algorithm. The real space integration grid had a cut-off of 500 Ry and up to 12000 points were used for the Brillouin zone sampling using the Monkhorst-Pack k-points sampling. Stringent criteria were adopted for the electronic structure convergence and equilibrium geometry (residual forces lower than  $10^{-2}$  eV/Å).

Our results are in close agreement with previous band structure calculations reported in Ref. 15. We find that Fe magnetic moment decreases with Ru doping and eventually vanishes for  $x$  around 0.5. This trend is qualit-

tatively consistent with the one experimentally derived from the  $x$  dependence of  $B_1^\mu(T \rightarrow 0, x)$  (Fig.3). Nevertheless, as it has already been pointed out in the introduction, band structure calculations do not provide a quantitatively correct estimate of the magnitude of Fe magnetic moment, as well as of the  $x$ -dependence of the order parameter. Namely, the initial slope  $d < S(T \rightarrow 0, x) > /dx$  obtained experimentally is much faster than the one derived from band structure calculations.

On the other hand, a better agreement with the experimental findings is observed for the calculated density of states at the Fermi level. This quantity can be derived experimentally from  $1/T_1$  measurements.<sup>25</sup> In fact, above  $T_N$   $1/T_1$  follows the Korringa behaviour expected for a Fermi liquid (Fig.4), namely  $1/T_1 = Cn_0^2 T$ , with  $n_0$  the density of states at the Fermi level and  $C$  a constant accounting for the hyperfine coupling between the electrons and  $^{139}\text{La}$  nuclei. Then, by taking the value of the spin-lattice relaxation rate around room temperature one can write that  $\sqrt{T_1(0)/T_1(x)} \simeq n_0(x)/n_0(0)$  and derive the  $x$ -dependence of the density of states at the Fermi level. In Fig.6 this ratio is compared to the results obtained from *ab initio* calculations in the paramagnetic state. One observes that  $n_0(x)$  decreases with increasing Ru content, in excellent agreement with band structure calculations. This decrease should be associated with the larger extension of Ru  $d$  orbitals which leads to an enhanced delocalization of the electrons.

At low temperature, in the SDW phase, LaFeAsO nuclear spin-lattice relaxation can be described as the sum of two contributions, as suggested by Smerald *et al.*<sup>26</sup>

$$\frac{1}{T_1} = \frac{1}{T_1^{FL}} + \frac{1}{T_1^{SW}} , \quad (2)$$

where  $1/T_1^{FL} \propto T$  is a Fermi-gas like term arising from weakly correlated electrons which accounts for the low-temperature levelling of  $1/T_1 T$ , while  $1/T_1^{SW}$  is the one from a band with strongly correlated electrons where the Fermi surface nesting leads to the insurgence of the SDW phase.

At low temperature  $1/T_1^{SW}$  reduction is determined by the gap  $\Delta$  in the spin excitations. In fact, following Ref.26, taking into account that the experiments were performed on powders, one can write

$$\begin{aligned} \frac{1}{T_1^{SW}} &\simeq \frac{4\mathcal{A}_h^2 m_0^2 \hbar V^2 \gamma_N^2 \Delta^3}{3\pi^3 \chi_\perp^2 v_s^6} \Phi\left[\frac{K_B T}{\Delta}\right] = \\ &= \frac{4}{3} \mathcal{A}_h^2 \gamma_N^2 m_0^2 \hbar \alpha^2 \Delta^3 \Phi\left[\frac{K_B T}{\Delta}\right] \end{aligned} \quad (3)$$

where  $\Phi[x] = x^2 Li_1(e^{-1/x}) + x^3 Li_2(e^{-1/x})$

with  $Li_n(z)$  the  $n^{\text{th}}$  polylogarithm of  $z$ . In Eq.3  $\mathcal{A}_h$  is the hyperfine coupling between the longitudinal fluctuations of the Fe moment and the nuclear spin,  $\gamma_N$  is  $^{139}\text{La}$  gyromagnetic ratio,  $m_0$  the amplitude of the fluctuating moment, while  $\alpha = V/\chi_\perp v_s^3 \pi^{3/2}$ , with  $V$  the unit cell volume,  $v_s$  the average spin-wave velocity and

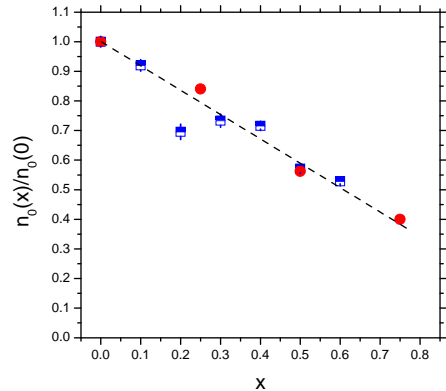


FIG. 6: The density of states at the Fermi level is reported as a function of Ru content in  $\text{LaFe}_{1-x}\text{Ru}_x\text{AsO}$ , normalized to the  $x = 0$  value. The squares represent the data derived from  $^{139}\text{La}$   $1/T_1$  measurements, while the circles are from band structure calculations. The dashed line is a guide to the eye.

$\chi_\perp$  the transverse spin susceptibility. It is interesting to observe that this approach applies also to the  $J_1 - J_2$  model on a square lattice with localized spins.<sup>27</sup> In fact, although  $\text{LaFe}_{1-x}\text{Ru}_x\text{AsO}$  is not a localized spin system, the  $J_1 - J_2$  model appears to be still applicable in some effective version also to the iron pnictides. Further support to this idea will be presented subsequently in the discussion of  $\text{LaFe}_{1-x}\text{Ru}_x\text{AsO}$  phase diagram.

It is interesting to notice that many parameters appearing in Eq.3 determine also the reduction of the sublattice magnetization. In fact one has that

$$\frac{< S >(0) - < S >(T)}{< S >(0)} = \alpha \sqrt{\Delta} \left( \frac{K_B T}{2} \right)^{3/2} e^{-\Delta/k_B T} \quad (4)$$

Thus, both the temperature dependence of  $< S >(T)$  and of  $1/T_1$  for  $T \ll T_N$  are determined by  $\Delta$ . By fitting ZF- $\mu$ SR and  $^{139}\text{La}$   $1/T_1$  curves for  $x = 0.1$  (Fig.7) one finds an accurate fit of both quantities for  $\Delta = 8 \pm 2$  meV, a value which is close to the one found in other iron pnictides by means of inelastic neutron scattering.<sup>28-30</sup> By assuming in Eq.3  $m_0 \simeq 1\mu_B$  one finds a quantitative agreement with  $^{139}\text{La}$   $1/T_1$  data for  $\mathcal{A}_h \simeq 1.8 \text{ kG}/\mu_B$ . This value is reasonably close to that estimated in the SDW phase from the hyperfine field at the  $^{139}\text{La}$  nucleus  $B_{La} \simeq 2.4 \text{ kG}$ . Namely, by assuming the  $T = 0$  value of the magnetic moment of Fe in the SDW phase<sup>31</sup> to be  $m = 0.6 \mu_B$ , one has  $\mathcal{A}_h \simeq |B_{La}|/z < M(0) > \simeq 1 \text{ kG}/\mu_B$ , with  $z = 4$  the nearest neighbor Fe atoms.

Further insights on the applicability of the  $J_1-J_2$  model to  $\text{LaFe}_{1-x}\text{Ru}_x\text{AsO}$  comes from the analysis of the phase diagram. As it is shown in Fig.8 the Néel temperature determined either from transport or from ZF- $\mu$ SR by taking the temperature at which  $v_M \rightarrow 1$  (Fig. 2), decreases almost linearly with  $x$  and eventually vanishes around  $x = 0.6$ . It may be argued that  $x \neq 0$  samples present a distribution of Néel temperatures and that the criteria chosen for identifying  $T_N$  may vary with the determination technique. Still, if we choose, for example, to eval-

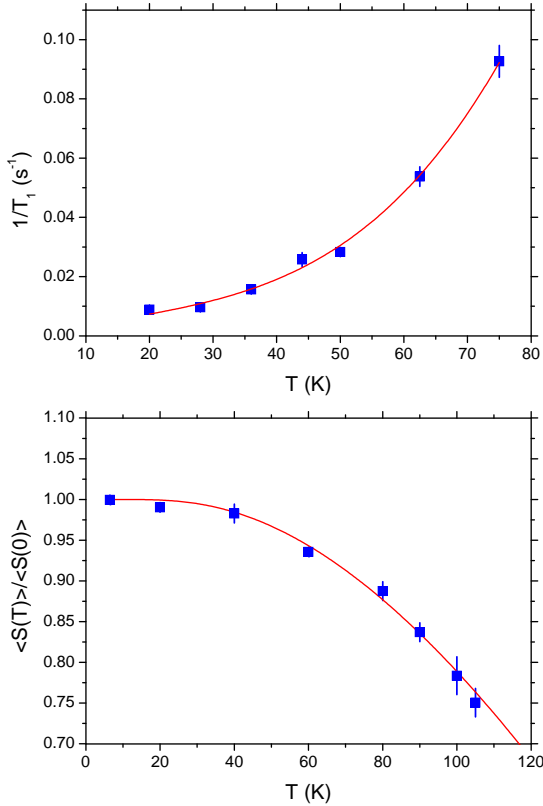


FIG. 7: (Top) Temperature dependence of  $^{139}\text{La}$   $1/T_1$  in  $\text{LaFe}_{0.9}\text{Ru}_{0.1}\text{AsO}$ , in a 7 Tesla magnetic field, for  $T \ll T_N$ . The solid line shows the best fit according to Eq.3. (Bottom) Temperature dependence of the magnetic order parameter derived from ZF- $\mu\text{SR}$  measurements. The solid line is the best fit according to Eq.4.

ate the average  $T_N^{av}$  from the flex in the muon magnetic fraction  $v_m(T)$ , the slope  $dT_N^{av}/dx$  turns out to be the same as that of Fig. 8. This points out that our main findings are not affected by some distribution in the Néel temperatures.

Now, it is instructive to compare the slope  $dT_N(x)/dx$  with the one found in  $\text{Li}_2\text{V}_{1-x}\text{Ti}_x\text{SiO}_5$ , a prototype of the  $J_1 - J_2$  model on a square lattice with spin dilution arising from the substitution of  $\text{V}^{4+}$  ( $S = 1/2$ ) with  $\text{Ti}^{4+}$  ( $S = 0$ ). One notices that the trend of  $T_N(x)/T_N(0)$  is the same in  $\text{LaFe}_{1-x}\text{Ru}_x\text{AsO}$  and  $\text{Li}_2\text{V}_{1-x}\text{Ti}_x\text{SiO}_5$ , further supporting the idea that the  $J_1 - J_2$  model on a square lattice<sup>16</sup> provides an effective framework to appropriately describe the effects of the spin dilution induced by Ru for Fe substitution.<sup>32</sup> Moreover, it is pointed out that in  $\text{LaFe}_{1-x}\text{Ru}_x\text{AsO}$   $T_N(x)$  vanishes for  $x$  around 0.6 which corresponds to the percolation threshold for the  $J_1 - J_2$

model on a square lattice.

#### IV. CONCLUSIONS

In conclusion, we have shown that Ru for Fe substitution in  $\text{LaFe}_{1-x}\text{Ru}_x\text{AsO}$  causes a progressive reduction of the Néel temperature ( $T_N$ ) and of the magnetic order pa-

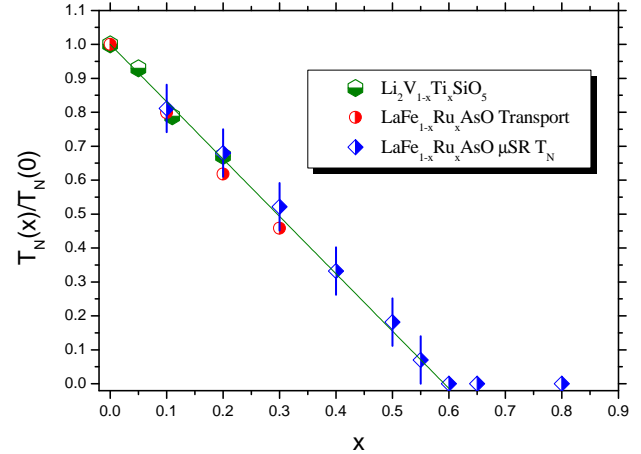


FIG. 8: The doping dependence of Néel temperature in  $\text{LaFe}_{1-x}\text{Ru}_x\text{AsO}$ , normalized to its  $x = 0$  value is shown. Circles show the behaviour derived from transport data, squares from ZF- $\mu\text{SR}$ , while diamonds show the corresponding behaviour for  $\text{Li}_2\text{V}_{1-x}\text{Ti}_x\text{SiO}_5$ .

rameter without leading to the onset of superconductivity. The analysis of  $^{139}\text{La}$  nuclear spin-lattice relaxation rate  $1/T_1$  indicates that this system can be described within a two-band model, one of them giving rise to the spin density wave (SDW) ground-state. Fe for Ru substitution yields to a progressive decrease of the density of states at the Fermi level in quantitative agreement with band structure calculations. The behaviour of  $1/T_1$  in the SDW phase and the reduction of  $T_N$  with Ru substitution can both be described within the  $J_1 - J_2$  model on a square lattice which suggests that  $\text{LaFe}_{1-x}\text{Ru}_x\text{AsO}$  behaves as a spin-diluted system with competing exchange interactions, pointing out the relevant role of frustration in the parent compounds of iron based superconductors.

The assistance by Alex Amato during the  $\mu\text{SR}$  measurements at PSI and the access support by EU contract RII3-CT-2003-505925 (NMI3) are gratefully acknowledged.

<sup>1</sup> Y. Kamihara, T. Watanabe, M. Hirano, and H. Hosono, *J. Am. Chem. Soc.* **130**, 3296 (2008)

<sup>2</sup> I. Mazin, D. Singh, M. Johannes and M. Du, *Phys. Rev. Lett.* **101**, 57003 (2008).

<sup>3</sup> H. Luetkens, H.H. Klauss, M. Kraken, F. J. Litterst,

T. Dellmann, R. Klingeler, C. Hess, R. Khasanov, A. Amato, C. Baines, M. Kosmala, O.J. Schumann, M. Braden, J. Hamann-Borrero, N. Leps, A. Kondrat, G. Behr, J. Werner, and B. Büchner, *Nature materials* **8**, 305 (2009).

<sup>4</sup> H.-H. Klauss, H. Luetkens, R. Klingeler, C. Hess, F. Litterst, M. Kraken, M. Korshunov, I. Eremin, S.-L. Drechsler, R. Khasanov, et al., Phys. Rev. Lett. **101**, 77005 (2008).

<sup>5</sup> T. Yildirim, Phys. Rev. Lett. **101**, 57010 (2008).

<sup>6</sup> Q. Si and E. Abrahams, Phys. Rev. Lett. **101**, 76401 (2008).

<sup>7</sup> C. de la Cruz, Q. Huang, J. W. Lynn, J. Li, W. Ratcliff, J. L. Zarestky, H. A. Mook, G. F. Chen, J. L. Luo, N. L. Wang, et al., Nature **453**, 899 (2008).

<sup>8</sup> H. Luetkens, H.-H. Klauss, R. Khasanov, A. Amato, R. Klingeler, I. Hellmann, N. Leps, A. Kondrat, C. Hess, A. Köhler, et al., Phys. Rev. Lett. **101**, 097009 (2008)

<sup>9</sup> H. Okada, K. Igawa, H. Takahashi, Y. Kamihara, M. Hirano, H. Hosono, K. Matsabayashi, and Y. Uwatoko, J. Phys. Soc. Jpn. **77**, 3712 (2008)

<sup>10</sup> S. Sharma, A. Bharathi, S. Chandra, V.R. Reddy, S. Paulraj, A.T. Satya, V.S. Sastry, A. Gupta and C.S. Sundar, Phys. Rev. B **81**, 174512 (2010).

<sup>11</sup> W. Schnelle, A. Leithe-Jasper, R. Gumeniuk, U. Burkhardt, D. Kasinathan and H. Rosner, Phys. Rev. B **79**, 214516 (2009)

<sup>12</sup> F. Rullier-Albenque, D. Colson, A. Forget, P. Thuéry, and S. Poissonnet, Phys. Rev. B **81**, 224503 (2010).

<sup>13</sup> A. Thaler, N. Ni, A. Kracher, J. Q. Yan, S. L. Bud'ko, and P. C. Canfield, Phys. Rev. B **82**, 014534 (2010).

<sup>14</sup> M.A. McGuire, D.J. Singh, A.S. Sefat, B.C. Sales, and D. Mandrus, J. of Solid State Chem. **182**, 2326 (2009).

<sup>15</sup> M. Tropeano, M. R. Cimberle, C. Ferdeghini, G. Lamura, A. Martinelli, A. Palenzona, I. Pallecchi, A. Sala, I. Sheikin, F. Bernardini, M. Monni, S. Massidda, and M. Putti, Phys. Rev. B **81**, 184504 (2010).

<sup>16</sup> D. C. Johnston, R. J. McQueeney, B. Lake, A. Honecker, M. E. Zhitomirsky, R. Nath, Y. Furukawa, V. P. Antropov, and Yogesh Singh, Phys. Rev. B **84**, 094445 (2011)

<sup>17</sup> I. Pallecchi, F. Bernardini, M. Tropeano, A. Palenzona, A. Martinelli, C. Bernini, C. Ferdeghini, M. Vignolo, S. Massidda, M. Putti, arXiv:1106.3973v1 (Unpublished).

<sup>18</sup> H. Takenaka and D. Singh, Phys. Rev. B **78**, 052503 (2008)

<sup>19</sup> H. Maeter, H. Luetkens, Y. Pashkevich, A. Kwadrin, R. Khasanov, A. Amato, A. Gusev, K. Lamonova, D. Chervinskii, R. Klingeler, et al., Phys. Rev. B **80**, 094524 (2009)

<sup>20</sup> A. Amato, Rev. Mod. Phys. **69** (1997).

<sup>21</sup> K. Ishida, Y. Nakai, S. Kitagawa, Y. Kamihara, M. Hirano, and H. Hosono, Physica B: Condensed Matter **404**, 3089 (2009).

<sup>22</sup> A. Suter, M. Mali, J. Roos, and D. Brinkmann, J. Phys. Condensed Matter **10**, 5977 (1998).

<sup>23</sup> Y. Nakai, K. Ishida, Y. Kamihara, M. Hirano, H. Hosono, J. Phys. Soc. Jpn. **77**, 073701 (2008)

<sup>24</sup> J.M. Soler, E. Artacho, J.D. Gale, A. García, J. Junquera, P. Ordejón, and D. Sánchez-Portal, J. Phys.: Condens. Matter, **14**, 2745 (2002).

<sup>25</sup> C. Slichter in *Principles of Magnetic Resonance 3<sup>rd</sup> Ed.*, Springer Verlag-Berlin (1990).

<sup>26</sup> A. Smerald and N. Shannon, EPL **92**, 47005 (2010); A. Smerald and N. Shannon, arXiv:1109.0384v1

<sup>27</sup> A. Smerald, private communication

<sup>28</sup> R. McQueeney, S. Diallo, V. Antropov, G. Samolyuk, C. Broholm, N. Ni, S. Nandi, M. Yethiraj, J. Zarestky, J. Pulikkotil, et al., Phys. Rev. Lett. **101**, 227205 (2008).

<sup>29</sup> J. Zhao, D.-X. Yao, S. Li, T. Hong, Y. Chen, S. Chang, W. Ratcliff, J. Lynn, H. Mook, G. Chen, et al., Phys. Rev. Lett. **101**, 167203 (2008).

<sup>30</sup> K. Matan, R. Morinaga, K. Iida, and T. Sato, Phys. Rev. B **79**, 054526 (2009).

<sup>31</sup> N. Qureshi, Y. Drees, J. Werner, S. Wurmehl, C. Hess, R. Klingeler, B. Büchner, M. T. Fernández-Díaz, and M. Braden, Phys. Rev. B **82**, 184521 (2010)

<sup>32</sup> N. Papinutto, P. Carretta, S. Gonthier, and P. Millet, Phys. Rev. B **71**, 174425 (2005).